Purdue University

Purdue e-Pubs

Department of Computer Science Technical Reports | Department of Computer Science

1996

Towards the Determination of the Optimal p-Cyclic SSOR

A. Hadjidimos

D. Noutsos

M. Tzoumas

Report Number:

96-079

Hadjidimos, A.; Noutsos, D.; and Tzoumas, M., "Towards the Determination of the Optimal p-Cyclic SSOR" (1996). *Department of Computer Science Technical Reports.* Paper 1333.
https://docs.lib.purdue.edu/cstech/1333

This document has been made available through Purdue e-Pubs, a service of the Purdue University Libraries.
Please contact epubs@purdue.edu for additional information.

TOWARDS THE DETERMINATION OF THE OPTIMAL p-CYCLIC SSOR

A. Hadjidimos
D. Noutsos
M. Tzoumas

CSD-TR 96-079
December 1996

Towards the Determination of the Optimal p–Cyclic SSOR

A. Hadjidimos[1] D. Noutsos[2] and M. Tzoumas[2]
Computer Science Department
Purdue University
West Lafayette, IN 47907

Abstract

Suppose that $A \in \mathbb{C}^{n,n}$ is a block p–cyclic consistently ordered matrix and let B and S_ω denote the block Jacobi and the block Symmetric Successive Overrelaxation (SSOR) iteration matrices associated with A, respectively. Extending previous work by Hadjidimos and Neumann, the present authors have determined the exact regions of convergence of the SSOR method in the $(\rho(B), \omega)$–plane, for any $p \geq 3$, under the further assumption that the eigenvalues of B^p are real of the same sign. In the present work the investigation goes on further, several questions are raised and among others the problem of the determination of the optimal regions of convergence in the spirit of Niethammer and Varga as well as that of the optimal relaxation factor are examined.

AMS (MOS) Subject Classifications: Primary 65F10. CR Categories 5.14.

Key Words: iterative method, symmetric successive overrelaxation, p–cyclic consistently ordered matrix, conformal mapping

Running Title: Optimal SSOR

[1]This work was supported by NSF grant CCR 86–19817, AFSOR grant 91–F49620, ARPA grant DAAH 04–94–G–0010.

[2]Department of Mathematics, University of Ioannina, GR-451 10 Ioannina, Greece.

1 Introduction

Given the nonsingular linear system

$$Ax = b \tag{1.1}$$

where $A \in \mathbb{C}^{n,n}$ and $x, b \in \mathbb{C}^n$. Suppose that A is written in the $p \times p$ block form

$$A = D(I - L - U) \tag{1.2}$$

with D being a $p \times p$ block diagonal invertible matrix, $p \geq 3$, and L and U being block strictly lower and strictly upper triangular matrices, respectively. Suppose also that for the solution of (1.1)–(1.2) the Symmetric Successive Overrelaxation (SSOR) iterative method (see, e.g., [24], [28], [1]) defined by

$$\begin{aligned} x^{(m+1/2)} &= (I - \omega L)^{-1}[(1-\omega)I + \omega U]x^{(m)} + \omega(I - \omega L)^{-1}D^{-1}b \ , \\ x^{(m+1)} &= (I - \omega U)^{-1}[(1-\omega)I + \omega L]x^{(m+1/2)} + \omega(I - \omega U)^{-1}D^{-1}b, \qquad m = 1, 2, \ldots, \end{aligned} \tag{1.3}$$

where $x^{(0)} \in \mathbb{C}^n$ arbitrary and $\omega \in (0, 2)$ the relaxation factor, is to be used. The block SSOR iteration matrix, associated with A, relative to its block partitioning, is given by

$$S_\omega := (I - \omega U)^{-1}[(1-\omega)I + \omega L](I - \omega L)^{-1}[(1-\omega)I + \omega U]. \tag{1.4}$$

Let $B := L + U$ be the block Jacobi matrix associated with A. If A is block p–cyclic consistently ordered then, without loss of generality, we may assume that B has the block form

$$B = \begin{bmatrix} 0 & 0 & 0 & \ldots & 0 & B_1 \\ B_2 & 0 & 0 & \ldots & 0 & 0 \\ 0 & B_3 & 0 & \ldots & 0 & 0 \\ \vdots & & & & & \\ 0 & 0 & 0 & \ldots & B_{p-1} & 0 \end{bmatrix}. \tag{1.5}$$

It is well known that the sets of eigenvalues μ of B (or of B^T) and λ of S_ω satisfy the functional equation

$$[\lambda - (1-\omega)^2]^p = \lambda(\lambda + 1 - \omega)^{p-2}(2-\omega)^2\omega^p\mu^p \tag{1.6}$$

which was discovered by Varga, Niethammer and Cai [25] and which generalized the corresponding relationship for $p = 2$ (see [2], [17]).

For the study of the convergence properties of the SSOR method any information about the spectrum of B, $\sigma(B)$, may enable one to answer one or more of the following questions:

i) For what pairs $(\rho(B), \omega)$ does (1.3) converge ($\rho(S_\omega) < 1$) and for what pairs $(\rho(B), \omega)$ does (1.3) converge in the sense of Niethammer and Varga (namely that $\rho(S_\omega) \leq \frac{1}{\eta}$, for a given $\eta \geq 1$)?

ii) What is the largest region, in the complex plane, that contains $\sigma(B)$ for which (1.3) converges in the sense of Niethammer and Varga as in (i) previously? and

iii) What is the (optimal) value of ω that minimizes $\rho(S_\omega)$ for a given $\rho(B)$ and what is the (optimal) region in the complex plane that contains a given $\sigma(B)$?

Complete answers to the first part of question (i) have been given by Neumaier and Varga [18] for the entire class of H–matrices, by Hadjidimos and Neumann [9] for consistently ordered matrices, and [10] for the class of p–cyclic matrices, and by Hadjidimos, Noutsos and Tzoumas [12] for the class of p–cyclic matrices with $\sigma(B^p)$ real of the same sign. An answer to question (ii) was given by Galanis, Hadjidimos and Noutsos [7] for $p = 2$ only. Finally, an answer to the first part of question (iii) was given by D'Sylva and Miles [2] and by Lynn [17] and, in a more general case but always for $p = 2$, by Hadjidimos and Noutsos [11]. In the latter work an algorithm of Young–Eidson's type was also presented for the determination of the optimal relaxation factor ω. It seems that for $p \geq 3$ the problems in the second part of question (i) and in questions (ii) and (iii) have not been studied so far. On the other hand, the corresponding problems in the simpler case of the p–cyclic SOR method have been extensively studied and a rich literature on them already exists. Here we mention some of the researchers in this area and refer to their works although the list we give is far from being exhausted; Young [27] (see also [28]), Varga [23] (see also [24]), Kredell [16], Niethammer [19], Young and Eidson [29] (see also [28]), Niethammer and Varga [21], Niethammer, dePillis and Varga [20], Hadjidimos, Li and Varga [8], Galanis, Hadjidimos and Noutsos [4], [5], [6], Wild and Niethammer [26] Eiermann, Niethammer and Ruttan [3], Kontovasilis, Plemmons and Stewart [15], Hadjidimos and Plemmons [13], Noutsos [22] et al.

In most of the works on both the p-cyclic SOR and SSOR methods conformal mapping transformations in the complex plane are extensively used where the region containing $\sigma(B)$ is related to a disk containing the spectrum of the SOR or the SSOR iteration matrices, respectively.

In the present work we try to give answers to the questions, raised previously, for the p–cyclic consistently ordered SSOR case for $p \geq 3$. The main tool to be used will be the theory of conformal mappings (see, e.g., [14]). Here, the reader is reminded that in the analysis in [12] parts of the exact boundaries could not be given analytically and had therefore to be determined computationally. Bearing in mind that the regions in [12] correspond to the value of the parameter $\eta = 1$ while in the present work this parameter can be practically any number $\eta > 1$ we must expect that some of the analogous results here can be found only computationally.

The organization of this paper is as follows. In Section 2, the mapping that connects the spectra involved in (1.6) is introduced. Next, the conditions under which the mapping considered is conformal are investigated and general conclusions regarding the spectra involved are drawn. Then, in Section 3, the study of the (optimal) regions of convergence and of the (optimal) relaxation factor ω is made and general results are obtained. Finally, in Section 4, the special case $p = 3$ is treated separately while in Section 5 some numerical results to support the theory developed are presented.

2 Conformal Mappings of the SSOR Spectral Regions

We begin our analysis with the functional equation (1.6) which is rewritten as follows

$$\mu^p = \frac{[\lambda - (1-\omega)^2]^p}{(2-\omega)^2\omega^p\lambda(\lambda+1-\omega)^{p-2}}. \tag{2.1}$$

Using the transformation

$$\phi = \frac{1}{\lambda}, \tag{2.2}$$

substituting into (2.1) and setting $z = \mu^p$, we obtain the mapping

$$z:\ z(\phi) = \frac{[1-(1-\omega)^2\phi]^p}{(2-\omega)^2\omega^p\phi[1+(1-\omega)\phi]^{p-2}}. \tag{2.3}$$

Our objective is to find the smallest region in the complex plane containing $\mu^p \in \sigma(B^p)$ which has an image, through the mapping (2.3), in the exterior of the circle

$$\partial D_\eta := \{\phi : \phi = \eta e^{i\theta},\ \eta > 0,\ \theta \in [0, 2\pi)\}, \tag{2.4}$$

where D_η is the corresponding disk, or, since $\lambda = \frac{1}{\eta}e^{-i\theta}$, in the interior of the circle $\partial D_{\frac{1}{\eta}}$. Then, the spectral radius of the SSOR iteration matrix will be less than or equal to $\frac{1}{\eta}$ ($\rho(S_\omega) \le \frac{1}{\eta}$) with equality holding if and only if (*iff*) there is an eigenvalue of B^p on the boundary of the region to be found.

For the solution of this problem we study the mapping (2.3) as η increases continuously from the value 0. First, we will try to find the conditions under which the mapping in question is conformal.

For $\eta = 0$ the circle ∂D_η is trivially the point 0 of the complex plane. So, (2.3) transforms the point 0 onto the point ∞ and the mapping is conformal. Due to the continuity of the mapping as η varies, it will be conformal for some $\eta > 0$ in the neighborhood of 0. As is known, a mapping like (2.3) is not conformal if there is a $\phi \in D_\eta$ such that $\frac{dz}{d\phi} = 0$. This suggests that the smallest value of η, for which $\frac{dz}{d\phi} = 0$ for some $\phi \in \partial D_\eta$, must be found.

Considering ω constant and differentiating (2.3) with respect to (*wrt*) ϕ, we can obtain after some simple manipulation that

$$\frac{dz}{d\phi} = 0 \iff F(\phi) = 0 \tag{2.5}$$

where

$$F(\phi) := (1-\omega)^3\phi^2 + (p-1)(1-\omega)(2-\omega)\phi + 1. \tag{2.6}$$

By considering the discriminant of the quadratic in (2.6) it is readily checked that $F(\phi)$ has only real zeros. Since $\phi = \eta e^{i\theta}$, the possible (real) zeros of (2.6) must correspond to $\theta = 0$ and $\theta = \pi$. Therefore we have to distinguish two cases which are studied in the sequel.

Case 1: For $\theta = 0$, (2.5)-(2.6) give

$$(1-\omega)^3\eta^2 + (p-1)(1-\omega)(2-\omega)\eta + 1 = 0 \tag{2.7}$$

and our problem turns out to be the determination of the smallest positive root of (2.7). Obviously, $\omega \neq 1$ because for $\omega = 1$, (2.7) cannot hold. The two roots of (2.7) are given by

$$\eta_{+,-} = \frac{-(p-1)(1-\omega)(2-\omega) \pm |1-\omega|[(p-1)^2(2-\omega)^2 + 4(\omega-1)]^{\frac{1}{2}}}{2(1-\omega)^3}. \tag{2.8}$$

For $\omega < 1$, both roots in (2.8) are negative and therefore the mapping is conformal. For $\omega > 1$, (2.8) gives

$$\eta_{-} = \frac{-(p-1)(2-\omega) + [(p-1)^2(2-\omega)^2 + 4(\omega-1)]^{\frac{1}{2}}}{2(1-\omega)^2}. \tag{2.9}$$

So, for $\eta \leq \eta_-$ the mapping is conformal while for $\eta > \eta_-$ it is not. In the latter case the image of the circle ∂D_η of the mapping (2.3) has an intersection (double) point on the real axis.

Case 2: For $\theta = \pi$, we have

$$(1-\omega)^3\eta^2 - (p-1)(1-\omega)(2-\omega)\eta + 1 = 0. \tag{2.10}$$

The two roots of (2.10) are given by

$$\eta_{+,-} = \frac{(p-1)(1-\omega)(2-\omega) \pm |1-\omega|[(p-1)^2(2-\omega)^2 + 4(\omega-1)]^{\frac{1}{2}}}{2(1-\omega)^3}. \tag{2.11}$$

For $\omega < 1$, the smallest positive root of (2.10) is

$$\eta_{-} = \frac{(p-1)(2-\omega) - [(p-1)^2(2-\omega)^2 + 4(\omega-1)]^{\frac{1}{2}}}{2(1-\omega)^2}. \tag{2.12}$$

The value $\eta = \eta_-$ just found is the only value of η at which the mapping (2.3) ceases to be conformal. This is because, as we saw before, for $\theta = 0$ the mapping is always conformal. For $\omega > 1$, the positive root of (2.10) is

$$\eta_- = \frac{(p-1)(2-\omega) + [(p-1)^2(2-\omega)^2 + 4(\omega-1)]^{\frac{1}{2}}}{2(1-\omega)^2}. \tag{2.13}$$

In order to find the value of η at which the mapping ceases to be conformal we compare the value $\eta = \eta_-$ found in (2.13) with the one corresponding to $\theta = 0$ and given in (2.9). Obviously, the smallest of the two $\eta's$ is the one corresponding to $\theta = 0$. Here we note that the value of η in (2.13) is greater than $\frac{1}{(1-\omega)^2}$ and because for $\eta = \frac{1}{(1-\omega)^2}$ and $\theta = 0$, z in (2.3) reduces to zero it is implied that there exists no convergence region for the SSOR method for $\eta > \frac{1}{(1-\omega)^2}$. This is not unexpected since, as is known from the analog to the Kahan Theorem for the SOR method, for the SSOR method $\rho(S_\omega) \geq (1-\omega)^2$ holds (see, e.g., [28]). Therefore, the value of η in (2.13) is of no interest.

The analysis above leads us to the following conclusion.

Theorem 2.1. The transformation (2.3) maps the circle ∂D_η in (2.4) into a closed curve C_p in the complex plane. For $\omega > 1$, this mapping is conformal for all

$$\eta \in (0, \hat{\eta}], \quad \hat{\eta} = \frac{-(p-1)(2-\omega) + [(p-1)^2(2-\omega)^2 + 4(\omega-1)]^{\frac{1}{2}}}{2(1-\omega)^2} \; \left(< \frac{1}{(1-\omega)^2} \right) \tag{2.14}$$

and is not conformal otherwise, while for $\omega < 1$, the mapping is conformal for all

$$\eta \in (0, \tilde{\eta}], \quad \tilde{\eta} = \frac{(p-1)(2-\omega) - [(p-1)^2(2-\omega)^2 + 4(\omega-1)]^{\frac{1}{2}}}{2(1-\omega)^2} \; \left(< \frac{1}{(1-\omega)^2} \right) \tag{2.15}$$

and is not conformal otherwise.

The theorem just presented and well known properties of Complex Analysis (see, e.g., [14]) give us the statement below.

Corollary 2.2. For the values of η of Theorem 2.1 for which the mapping (2.3) is conformal, (2.3) maps the interior of the disk $D_\eta = \{\phi : |\phi| \leq \eta\}$ onto the exterior of the closed simple curve C_p.

Remark: The curve C_p is symmetric *wrt* the real axis. This is readily checked by comparing the expressions in (2.3) for $\phi = \eta e^{i\theta}$ and $\phi = \eta e^{-i\theta}$.

3 Optimal Regions of Convergence

The analysis in the previous section provides us with the main tool for the study of the (optimal) convergence properties of the SSOR iterative method. Since $\frac{1}{\eta}$ is the spectral radius of the SSOR iteration matrix, in order to have convergence there must hold $\eta > 1$.

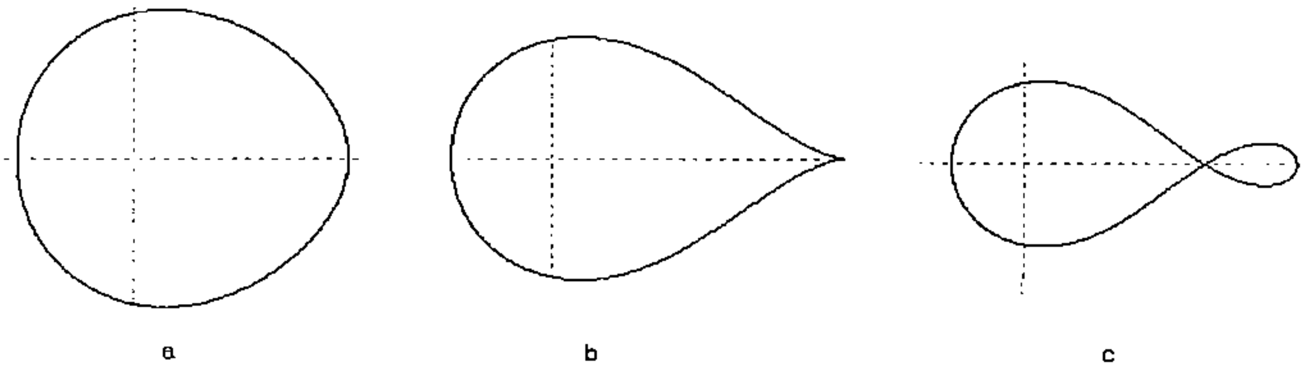

Figure 1: Regions of Convergence

For $\omega = 1$ (Aitken's method) the curve C_p is the circle $\frac{1}{\eta}e^{-i\theta}$ and the mapping is conformal for all η. So, in the sequel we distinguish two cases, depending on whether ω is greater or less than 1.

Case 1: $\omega \in (1,2)$

To study the mapping (2.3), we take a certain $\omega \in (1,2)$ and increase continuously the value of η starting from $\eta = 0$. For $\eta = 0$, (2.3) maps the point 0 of the complex plane onto ∞. For $0 < \eta < \widehat{\eta}$, it maps the disk D_η onto the exterior of the curve C_p and the mapping is conformal. This means that the curve C_p is a simple closed curve containing the point 0 of the complex plane in its interior. Moreover, for $\eta > 1$, the interior of C_p, let Ω denote it, is such that if $\sigma(B^p) \in \Omega$ then the associated SSOR method will converge with an asymptotic convergence factor $\rho(S_\omega)$ ($\leq \frac{1}{\eta}$). The region of convergence Ω is shown in Figure 1a for $p = 4$, $\omega = 1.2$ and $\eta = 1.1$. It is obvious that the larger η is the smaller the region Ω is.

For $\eta = \widehat{\eta}$, we have the largest value of η for which the mapping is conformal. The corresponding convergence region Ω is shown in Figure 1b for $p = 4$, $\omega = 1.2$, as before, and $\eta \approx 2.01562$. As is seen, at $\theta = 0$ the curve C_p has a cusp. In analytical terms this means that the derivative of (2.3) *wrt* ϕ becomes zero at $\phi = \widehat{\eta}$ ($\frac{dz}{d\phi}|_{\phi=\widehat{\eta}} = 0$).

For $\widehat{\eta} < \eta < \frac{1}{\omega-1}$, the mapping is not conformal. As is shown in Figure 1c for $p = 4$, $\omega = 1.2$ and $\eta = 2.4$, there is an intersection (double) point of the curve C_p on the positive real semiaxis. For specific values of η the abscissa of this point can be found only computationally. Because of the fact that the mapping is not conformal it is very difficult to describe explicitly the images of all the subregions formed by the curve C_p for all possible values of ω and η. The only somehow general description one can give regarding the convergence region Ω mentioned previously is that it is the subregion formed by C_p that contains the point 0 of the complex plane in its interior and has its images in the exterior of the circle $\eta e^{i\theta}$. In the case of Figure 1c, Ω is the left of the two subregions formed by C_p.

For $\eta = \frac{1}{\omega-1}$, we have the same conclusions with the main difference that the point of C_p

corresponding to $\theta = 0$ goes to ∞. So, C_p is not a closed curve.

For $\frac{1}{\omega-1} < \eta < \frac{1}{(\omega-1)^2}$, the point of C_p corresponding to $\theta = 0$ lies in the negative real semiaxis for odd p while it is still on the positive real semiaxis for even p. The curve C_p is now more complicated in shape. For some $\eta's$ we have more than one intersection (double) points of the curve C_p with the real semiaxis and more intersection (double) points of C_p with itself. Because of the continuity of the mapping, the only thing that can be said is that the smallest subregion formed by C_p that contains the point 0 of the complex plane in its interior is the convergence region Ω, in the sense explained previously.

For $\eta = \frac{1}{(\omega-1)^2}$, the region of convergence reduces trivially to the point 0 of the complex plane.

For $\eta > \frac{1}{(\omega-1)^2}$, there exists no region of convergence for the SSOR method.

Case 2: $\omega \in (0, 1)$

In the present case, results analogous to the ones of the previous Case 1 can be obtained provided one follows step by step the analysis done there. The main differences are that the value $\tilde{\eta}$ takes the place of $\hat{\eta}$, the value $\frac{1}{1-\omega}$ replaces that of $\frac{1}{\omega-1}$ in the various intervals considered, and the roles of the positive and negative real semiaxes are interchanged.

Based on the analysis of this section we can state the following theorem.

Theorem 3.1. Let $\eta > 1$ be given and let Ω be the region defined in the previous analysis for a given $\omega \in (1 - \frac{1}{\sqrt{\eta}}, 1 + \frac{1}{\sqrt{\eta}})$. Let also that $\sigma(B^p) \subset \Omega$. Then, the associated SSOR method converges with a spectral radius $\rho(S_\omega) \leq \frac{1}{\eta}$. In the last relationship equality holds *iff* at least one element of $\sigma(B^p)$ lies on the boundary $\partial\Omega$ of Ω.

The analysis so far gives answers to the second part of question (i) as well as to question (ii) of the Introduction. In the following two subsections we shall try to answer questions (i) and (iii) under the assumption that the spectra $\sigma(B^p)$ are real of the same sign.

3.1 Nonnegative Case

In [12] we determined the regions of convergence of the SSOR method ($\rho(S_\omega) < 1$) in the $(\rho(B), \omega)$–plane (or, equivalently, $(\rho(B^p), \omega)$–plane) for nonnegative and nonpositive spectra $\sigma(B^p)$ for all $p \geq 3$. Here we will try to determine regions in the $(\rho(B^p), \omega)$–plane such that $\rho(S_\omega) \leq \frac{1}{\eta}$ for a given $\eta > 1$ and also, whenever possible, optimal values of the relaxation factor ω for a given $\rho(B)$.

For a given $\eta > 1$ we study the transformation (2.3) for all values of $\omega \in (0, 2)$. More specifically, in the present case we must determine the closest to the origin $O(0, 0)$ point of intersection of the curve C_p with the positive real semiaxis. In the sequel we distinguish subcases.

For $0 < \omega < 1 - \frac{1}{\sqrt{\eta}}$, it is obvious that no such region exists since then $\eta > \frac{1}{(1-\omega)^2}$.

For $1 - \frac{1}{\sqrt{\eta}} \leq \omega < 1$, it is easily checked that $|z|$ takes its minimum value at the point corresponding to $\theta = 0$. So, the closest to 0 point we are seeking is that corresponding to

$\theta = 0$.

For $1 \leq \omega < 1+\frac{1}{\sqrt{\eta}}$, it is known from the analysis of the previous section that for certain $\omega's$ there exists an $\widehat{\eta}$ such that the mapping (2.3) is not conformal for $\eta > \widehat{\eta}$. The question that arises is then the following: For the given value of η can one find an $\widehat{\omega}$ for which the mapping ceases to be conformal? To answer this question a further study of equation (2.6), where ω is to be considered now as the variable, must be made. Setting $x = 1 - \omega$, (2.6) becomes

$$f(x) := \eta^2 x^3 + (p-1)\eta x^2 + (p-1)\eta x + 1 = 0. \tag{3.1}$$

Since $f(0) = 1 > 0$ and $f(-\frac{1}{\eta}) = (p-2)(\frac{1}{\eta} - 1) < 0$, there are one or three roots of (3.1) in the interval $(-\frac{1}{\eta}, 0)$. By studying the sign of the derivative of f with respect to x as a function of x it is concluded that there is precisely one zero of f in the interval in question. This implies that there is precisely one value of ω, denoted by $\widehat{\omega}$, in the interval $(1, 1+\frac{1}{\sqrt{\eta}})$ for which the mapping ceases to be conformal. Since the mapping is conformal for $\omega = 1$, it will be conformal for all the values of ω such that $1 \leq \omega \leq \widehat{\omega}$.

For $\widehat{\omega} < \omega \leq 1+\frac{1}{\sqrt{\eta}}$, the mapping is not conformal and the closest to the origin intersection point of interest corresponds to a $\theta \neq 0$ that can be found only computationally. For this, one has to set $\mathrm{Im}z(\eta e^{i\theta}) = 0$, next solve for θ and then find the value of θ that gives the smallest positive $\mathrm{Re}z(\eta e^{i\theta})$.

For $1 + \frac{1}{\sqrt{\eta}} < \omega < 2$, it is $\eta > \frac{1}{(1-\omega)^2}$ and there exists no region of convergence for the SSOR method.

The analysis so far gives the boundary curve of the region of interest in the $(\rho(B^p), \omega)$–plane. For $1 - \frac{1}{\sqrt{\eta}} \leq \omega \leq \widehat{\omega}$, this boundary curve can be given analytically by putting $\theta = 0$ in (2.3). So, we obtain

$$\beta_1(\omega) = \frac{[1-(1-\omega)^2\eta]^p}{(2-\omega)^2\omega^p\eta[1+(1-\omega)\eta]^{p-2}}, \quad \omega \in [1 - \frac{1}{\sqrt{\eta}}, \widehat{\omega}]. \tag{3.2}$$

For $\widehat{\omega} < \omega < 1 + \frac{1}{\sqrt{\eta}}$, the corresponding boundary curve $\beta_2(\omega)$ can be found only computationally as was explained previously.

The above analysis gives an answer to the second part of question (i) of the Introduction and the corresponding region for $p = 4$ and $\eta = 1.5$ is shown in Figure 2.

To give an answer to question (iii), in other words to determine optimal values of ω, we must determine those $\omega's$ which maximize η for a given $\rho(B)$ or $\omega's$ that maximize $\rho(B)$ for a given η. In this sense we can use the above analysis to determine the desired optimal values. More specifically, we will try to determine ω^* such that

$$\beta(\omega^*) = \max_{\omega} \beta(\omega), \quad \omega \in (1 - \frac{1}{\sqrt{\eta}}, 1 + \frac{1}{\sqrt{\eta}}) \tag{3.3}$$

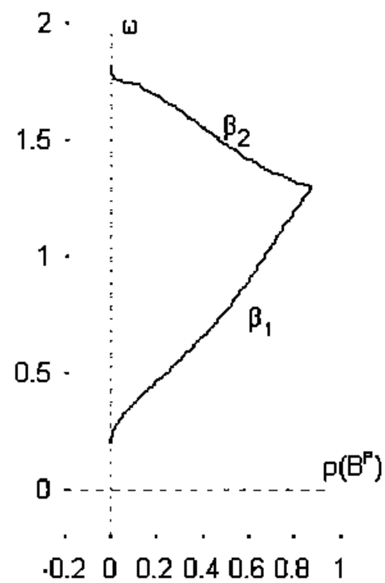

Figure 2: Convergence Region for the Nonnegative Case

where

$$\beta(\omega) = \begin{cases} \beta_1(\omega), & \omega \in (1 - \frac{1}{\sqrt{\eta}}, \hat{\omega}] \\ \beta_2(\omega), & \omega \in (\hat{\omega}, 1 + \frac{1}{\sqrt{\eta}}). \end{cases} \tag{3.4}$$

For this we must try to find the maximum values of the functions $\beta_1(\omega)$ and $\beta_2(\omega)$.

To study the function $\beta_1(\omega)$ first we differentiate it *wrt* ω and then use the transformation $x = 1 - \omega$. After some simple algebraic manipulation we obtain

$$\beta\prime_1(\omega) \sim (p-2)\eta x^3 + (p+2)\eta x^2 + (p+2)x + (p-2) =: f(x;\eta), \tag{3.5}$$

where a relationship of the form $A \sim B$ denotes that the two expressions or quantities A and B are of the same sign.

To find the sign of $f(x;\eta)$ for $x \in [1-\hat{\omega}, \frac{1}{\sqrt{\eta}})$ and $\eta \geq 1$ we work as follows. For $\eta = 1$, (3.5) gives

$$f(x;1) = (p-2)x^3 + (p+2)x^2 + (p+2)x + (p-2) = (x+1)[(p-2)x^2 + 4x + (p-2)]. \tag{3.6}$$

It is obvious that $f(x;1)$ has the simple zero -1 for all $p > 4$, the triple zero -1 for $p = 4$, and the zeros $-2-\sqrt{3}$, -1 and $-2+\sqrt{3}$ for $p = 3$. So, $f(x;1) > 0$, $\forall\, x \in [1-\hat{\omega}, \frac{1}{\sqrt{\eta}})$ and $p \geq 4$. For $p = 3$ the zero $-2+\sqrt{3}$ lies in the interval $[1-\hat{\omega}, \frac{1}{\sqrt{\eta}})$ for some values of η which means that $f(x;1)$ may change sign in this interval. Because of the fact that, for $p = 3$, $f(x;1)$ behaves in a different way this case will be examined separately in Section 4.

From (3.5)–(3.6) we have that

$$f(x;\eta) = f(x;1) + x^2(\eta - 1)[(p-2)x + (p+2)]. \tag{3.7}$$

Since for $p \geq 4$, both terms on the right hand side of (3.7) are greater than zero we have that

$$f(x;\eta) > 0, \ \forall\, x \in [1-\widehat{\omega}, \frac{1}{\sqrt{\eta}}). \tag{3.8}$$

This means that $\beta_1(\omega)$ is a strictly increasing function in $[1-\widehat{\omega}, \frac{1}{\sqrt{\eta}})$. Consequently

$$\max_{\omega} \beta_1(\omega) = \beta_1(\widehat{\omega}), \ \omega \in [1-\widehat{\omega}, \frac{1}{\sqrt{\eta}}). \tag{3.9}$$

Based on the above analysis we state and prove the following theorem.

Theorem 3.2. Let $p \geq 4$, $\sigma(B^p)$ be nonnegative and $\rho(B)$ (< 1) be given. Then there exists a unique root $\widehat{\omega} \in (1,2)$ of the equation

$$\rho(B^p) = \frac{\left[2+(p-1)(2-\omega)-\left[(p-1)^2(2-\omega)^2+4(\omega-1)\right]^{\frac{1}{2}}\right]^p}{2(2-\omega)^2\omega^p\left[-(p-1)(2-\omega)+\left[(p-1)^2(2-\omega)^2+4(\omega-1)\right]^{\frac{1}{2}}\right]} \times \frac{(1-\omega)^p}{\left[2(1-\omega)-(p-1)(2-\omega)+\left[(p-1)^2(2-\omega)^2+4(\omega-1)\right]^{\frac{1}{2}}\right]^{p-2}} \tag{3.10}$$

and the SSOR method converges for all $\omega \in (0, \widehat{\omega}]$ with $\widehat{\omega}$ being the optimal value of ω in this interval. The associated optimal spectral radius is

$$\rho(S_{\widehat{\omega}}) = \frac{1}{\widehat{\eta}}, \tag{3.11}$$

where $\widehat{\eta}$ is the value of η given by Theorem 2.1 provided $\widehat{\omega}$ replaces ω.

Proof: The convergence of the SSOR method ($\eta = 1$) was studied in [12]. From the theory developed so far we have that for a given $\widehat{\eta} > 1$ there exists a unique value of $\widehat{\omega} \in (1,2)$ given from the expression (2.14) of Theorem 2.1. From (3.2), the pair of values $\widehat{\omega}$ and $\widehat{\eta}$ corresponds to the largest $\rho(B)$. Conversely, for a given $\rho(B) < 1$ there exists a unique value $\widehat{\omega} \in (1,2)$ and a corresponding value for $\widehat{\eta}$ such that the convergence will be optimal for all $\omega \in (0, \widehat{\omega}]$. Equation (3.10) is thus obtained using the expressions for $\widehat{\omega}$ and $\widehat{\eta}$ in (3.2) and the proof of the present theorem is concluded. □

It remains to find the optimal value of ω in the interval $[\widehat{\omega}, 2)$. The theoretical analysis in this case becomes very complicated because of the intersection point(s) of C_p with the real positive semiaxis which correspond(s) to some $\theta \neq 0$. (The reader is reminded that this was exactly the case in [12] where $\eta = 1$.) Based on strong numerical evidence from a variety of numerical examples and computer graphics we have found out that in all the cases examined the function $\beta_2(\omega)$ behaves as a strictly decreasing one. After the observation just made a strong conjecture can be made; namely, that under the assumptions of Theorem 3.2 the optimal value of ω for all $\omega \in (0,2)$ is the unique value of $\hat{\omega} \in (1,2)$ given by equation (3.10).

3.2 Nonpositive Case

An analysis analogous to the one in the previous Section 3.1 of the nonnegative case can also be done here. For this, let $\eta > 1$ be given and let $\tilde{\omega} < 1$ be the value of ω at which the mapping (2.3) ceases to be conformal. Since for $\omega \in (\tilde{\omega}, \hat{\omega})$ the mapping is conformal we must study the behavior of the boundary curves of the region of interest in the intervals $(1 - \frac{1}{\sqrt{\eta}}, \tilde{\omega})$, $(\tilde{\omega}, \hat{\omega})$ and $(\hat{\omega}, 1 + \frac{1}{\sqrt{\eta}})$.

For $\omega \in (\tilde{\omega}, \hat{\omega})$, the boundary curve is given by putting $\theta = \pi$ in (2.3). Hence

$$\gamma_1(\omega) = |z(\eta e^{i\pi})| = \frac{[1 + (1-\omega)^2\eta]^p}{(2-\omega)^2\omega^p\eta[1-(1-\omega)\eta]^{p-2}}. \tag{3.12}$$

By differentiating $\gamma_1(\omega)$ *wrt* ω and then setting $x = 1 - \omega$ we obtain

$$\gamma\prime_1(\omega) \sim (p-2)\eta x^3 + (p+2)\eta x^2 - (p+2)x - (p-2) =: g(x;\eta). \tag{3.13}$$

It is readily found out that $g(-\infty;\eta) < 0$, $g(-\frac{1}{\sqrt{\eta}};\eta) > 0$, $g(\frac{1}{\sqrt{\eta}};\eta) < 0$, and $g(\infty;\eta) > 0$. Therefore, the cubic equation $g(x;\eta) = 0$ has precisely three real roots in the intervals $(-\infty, -\frac{1}{\sqrt{\eta}})$, $(-\frac{1}{\sqrt{\eta}}, 0)$ and $(\frac{1}{\sqrt{\eta}}, \infty)$, respectively. Obviously, only the second root, let us denoted it by $\overline{x}$, is of interest in the study of the behavior of the boundary curve. Consequently, there exists an $\overline{x} \in (-\frac{1}{\sqrt{\eta}}, 0)$, or an $\overline{\omega} \in (1, 1 + \frac{1}{\sqrt{\eta}})$, such that $\gamma_1(\omega)$ is a strictly decreasing function for $\omega \in (\tilde{\omega}, \overline{\omega})$ and a strictly increasing one for $\omega \in (\overline{\omega}, 1 + \frac{1}{\sqrt{\eta}})$.

The function $\gamma_1(\omega)$ defines the boundary curve for $\omega \in (\tilde{\omega}, \hat{\omega})$ and also, due to continuity, for an interval of ω $(\hat{\omega}, \hat{\hat{\omega}})$, where $\hat{\hat{\omega}} \in (\hat{\omega}, 1 + \frac{1}{\sqrt{\eta}})$ is the value of ω that corresponds to the closest to the origin intersection (double) point of the curve C_p, defined by $z(\eta e^{i\theta})$ in (2.3), with the real negative semiaxis. This point is obtained for some $\theta \neq \pi$. Moreover, from (3.13), $\gamma_1(\omega)$ attains a minimum at $\omega = \overline{\omega}$. The value $\hat{\hat{\omega}}$ can be found computationally in the general case while in Section 4 we will try to determine it in the special case $p = 3$. To establish the existence of $\hat{\hat{\omega}}$, we must prove that there exists an intersection point of the curve $z(\eta e^{i\theta})$ from (2.3) with the real negative semiaxis for some $\theta \neq \pi$ that is closer to the origin than the point corresponding to $\theta = \pi$. For this, we study the behavior of the argument of the complex number $\frac{1-(1-\omega)^2\eta e^{i\theta}}{1+(1-\omega)\eta e^{i\theta}}$ as $\eta \to \frac{1}{(1-\omega)^2}$ (or as $\omega \to 1 + \frac{1}{\sqrt{\eta}}$). For $\theta = 0$ the argument in question is 0 while as θ varies continuously taking on positive values in the neighborhood of 0 we claim that this argument tends to $-\frac{\pi}{2}$ very rapidly. To justify our claim, note that the argument of the numerator tends to $-\frac{\pi}{2}$ while the argument of the

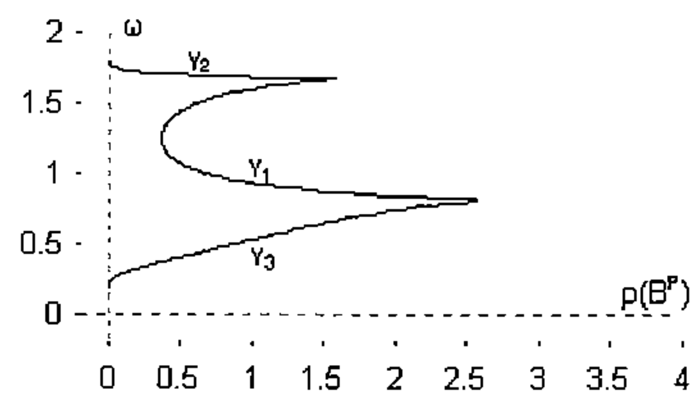

Figure 3: Convergence Region of the Nonpositive Case

denominator remains in the neighborhood of 0. So, by considering the p-th powers of the above complex number, since the other factor terms do not play any important role in the way the argument of $z(\eta e^{i\theta})$ varies for θ near 0, we have that: For small changes of θ from 0 to positive values the corresponding argument for points of the curve $z(\eta e^{i\theta})$ varies rapidly from 0 to $-\frac{p\pi}{2}$, via negative values. This means that for $\omega \to 1+\frac{1}{\sqrt{\eta}}$, there is an intersection point of the curve $z(\eta e^{i\theta})$ with the negative real semiaxis. The distance of this point from the origin tends also to 0. So, the existence of $\hat{\hat{\omega}} \in (\hat{\omega}, 1+\frac{1}{\sqrt{\eta}})$ is established. Moreover, this analysis effectively proves that the region Ω of $\sigma(B^p)$, studied in Section 2, reduces to the point of the origin as $\eta \to \frac{1}{(1-\omega)^2}$.

For $\omega \in (\hat{\hat{\omega}}, 1+\frac{1}{\sqrt{\eta}})$ the boundary curve $\gamma_2(\omega)$ can be found only computationally and has been shown by numerous numerical examples and computer graphics that it behaves as a strictly decreasing function.

It remains to study the case $\omega \in (1-\frac{1}{\sqrt{\eta}}, \tilde{\omega})$. As has been found out, the mapping is not conformal and the closest to the origin intersection point of interest can only be found computationally (a situation similar to the one in [12]). As is shown by a variety of numerical experiments and computer graphics, the boundary curve $\gamma_3(\omega)$ behaves as a strictly increasing function for all $p \geq 4$. The case $p=3$ is different and will be studied in Section 4. The region of interest in the $(\rho(B^p), \omega)$–plane for $p \geq 4$ is shown in Figure 3 for $p=4$ and $\eta = 1.5$.

From the previous analysis it is concluded that for $\omega \in (\tilde{\omega}, \hat{\hat{\omega}})$ there are two local maximum values of the curve $\gamma_1(\omega)$, if $\hat{\hat{\omega}} > \overline{\omega}$, corresponding to the points $\tilde{\omega}$ and $\hat{\hat{\omega}}$. The optimal value of ω is either $\tilde{\omega}$ or $\hat{\hat{\omega}}$ whichever corresponds to $max\{\gamma_1(\tilde{\omega}), \gamma_1(\hat{\hat{\omega}})\}$. Having in mind the results in [12] we can now state the following theorem which is analogous to Theorem 3.2 and its proof is a direct consequence of the analysis done so far.

Theorem 3.3. Let $p \geq 4$, $\sigma(B^p)$ be nonpositive, $\rho(B)$ be given and

$$\rho_i = \frac{1 + (1-\omega_i)^2}{(2-\omega_i)^{\frac{2}{p}} \omega_i^{2-\frac{2}{p}}}, \; i = 1, 2, \tag{3.14}$$

with

$$\omega_1 = \frac{2(p-2)^{\frac{1}{2}}}{(p+2)^{\frac{1}{2}} + (p-2)^{\frac{1}{2}}}, \quad \omega_2 = \frac{2(p-1)^{\frac{1}{2}}}{(p-1)^{\frac{1}{2}} + 1}. \tag{3.15}$$

Then, for any $\rho(B) < \rho_1$, there exists a unique root $\tilde{\omega} \in (0,1)$ of the equation

$$\rho(B^p) = \frac{\left[2+(p-1)(2-\omega)-\left[(p-1)^2(2-\omega)^2+4(\omega-1)\right]^{\frac{1}{2}}\right]^p}{2(2-\omega)^2\omega^p\left[(p-1)(2-\omega)-\left[(p-1)^2(2-\omega)^2+4(\omega-1)\right]^{\frac{1}{2}}\right]} \times \frac{(1-\omega)^p}{\left[2(1-\omega)-(p-1)(2-\omega)+\left[(p-1)^2(2-\omega)^2+4(\omega-1)\right]^{\frac{1}{2}}\right]^{p-2}} \tag{3.16}$$

and for any $\rho(B)$, unless $p \geq 15$ *and* $1 \leq \rho(B)$, there exists a unique value $\hat{\hat{\omega}}$ which is the smallest $\omega \in (1,2)$ such that there is an intersection point of the curve C_p at $(-\rho(B^p), 0)$ for a $\theta \neq \pi$. Furthermore, for any $p \geq 4$ and any $\rho(B)$ let $\tilde{\eta}$ (resp. $\hat{\hat{\eta}}$) denote the corresponding value of η; if both $\tilde{\omega}$ and $\hat{\hat{\omega}}$ exist let $\eta^* = max\{\tilde{\eta}, \hat{\hat{\eta}}\}$. Then, if $\tilde{\omega}$ (resp. $\hat{\hat{\omega}}$) exists there is always an interval of ω containing $\tilde{\omega}$ (resp. $\hat{\hat{\omega}}$) in which the SSOR method converges with local optimal spectral radius at $\omega^* = \tilde{\omega}$ (resp. $\omega^* = \hat{\hat{\omega}}$), namely $\rho(S_{\omega^*}) = \frac{1}{\tilde{\eta}}$ (resp. $\rho(S_{\omega^*}) = \frac{1}{\hat{\hat{\eta}}}$). Finally, for any $p \geq 4$ and any $\rho(B) \leq \rho_2$ the SSOR method converges for all ω in an interval containing both $\tilde{\omega}$ and $\hat{\hat{\omega}}$ with optimal spectral radius $\rho(S_{\omega^*}) = \frac{1}{\eta^*}$.

Note: One can be more specific about the intervals of convergence containing $\tilde{\omega}$ (resp. $\hat{\hat{\omega}}$) if one uses the theory in [9], [12], the preceding analysis and Theorem 3.3.

Based on strong numerical evidence from numerous numerical experiments and computer graphics we can make the strong conjecture that under the assumptions of Theorem 3.3, for all $\omega \in (0,2)$ the value of $\omega = \omega^*$ of Theorem 3.3 is the optimal value for the convergence of the SSOR method. Obviously, in the case where $\tilde{\omega}$ and $\hat{\hat{\omega}}$ exist in two disjoint intervals the one that corresponds to $\eta^* = max\{\tilde{\eta}, \hat{\hat{\eta}}\}$ is the optimal value of ω.

4 The Special Case $p = 3$

As has already been mentioned there are some basic differences regarding the regions of convergence and the optimal values in the special case $p = 3$ which is studied in this section.

From the analysis of Section 2 and especially from Theorem 2.1 and Corollary 2.2, for $p = 3$, we have that

$$\widehat{\eta} = \frac{-(2-\omega) + [(2-\omega)^2 + \omega - 1]^{\frac{1}{2}}}{(\omega-1)^2} \tag{4.1}$$

and

$$\widetilde{\eta} = \frac{(2-\omega) - [(2-\omega)^2 + \omega - 1]^{\frac{1}{2}}}{(\omega-1)^2}. \tag{4.2}$$

Below, following the analysis of Section 3 we shall try to find the boundary curves of the regions of convergence in the nonnegative and the nonpositive cases.

4.1 Nonnegative Case

For $\omega < 1$, the conclusions are the same as those of the general case. So, for $1 \leq \omega \leq 1 + \frac{1}{\eta}$ there exists an $\widehat{\omega}$ corresponding to $\widehat{\eta}$ such that for $\omega \leq \widehat{\omega}$ the mapping (2.3) is conformal while for $\omega > \widehat{\omega}$ it is not. Consequently, the boundary curve of the convergence region is that given in (3.4), where

$$\beta_1(\omega) = \frac{[1-(1-\omega)^2\eta]^3}{(2-\omega)^2\omega^2\eta[1+(1-\omega)\eta]}, \quad \omega \in \left[1 - \frac{1}{\sqrt{\eta}}, \widehat{\omega}\right] \tag{4.3}$$

and $\beta_2(\omega)$ can be found computationally. A number of experiments has shown that $\beta_2(\omega)$ behaves as a strictly decreasing function of ω as in the general case.

The behavior of $\beta_1(\omega)$, for $\omega \in [1, \widehat{\omega}]$ is to be studied in the sequel. From (3.5) we have that

$$\beta\prime_1(\omega) \sim \eta x^3 + 5\eta x^2 + 5x + 2 =: f_3(x;\eta) \tag{4.4}$$

It is obvious that $f_3(-\frac{1}{\eta};\eta) > 0$ and $f_3(0;\eta) > 0$. Differentiating $f_3(x;\eta)$ *wrt* x we have

$$f_{3}\prime(x;\eta) = 3\eta x^2 + 10\eta x + 5. \tag{4.5}$$

Since $f_3\prime(-\frac{1}{\eta};\eta) < 0$ and $f_3\prime(0;\eta) > 0$, $f_3\prime(x;\eta)$ has precisely one zero $\xi \in \left(-\frac{1}{\eta}, 0\right)$. So, $f_3(x;\eta)$ has none or two zeros in the same interval. By plugging in ξ in (4.4) we can find computationally that $f_3(\xi;\eta) < 0$ for $\eta \in [1, 1.3615345)$. This implies that for all $\eta's$ in the interval just found $f_3(x;\eta)$ has two zeros in $\left(-\frac{1}{\eta}, 0\right)$. The question that arises is which one of the two zeros belongs to the subinterval $(\widehat{x}, 0)$, where $\widehat{x} = 1 - \widehat{\omega}$. To answer this question we will try to find the value of η such that $\widehat{x}$ is one of the two aforementioned zeros. By applying the Sylvester's resolvent to the equation $f_3\prime(x;\eta) = 0$ and to equation (2.7) for $p = 3$, we readily obtain that $\widehat{x}$ can be a common root of these two equations only if $\eta = 1$. This implies that for all $\eta \in [1, 1.3615345)$ the two zeros belong to the interval $(\widehat{x}, 1)$. This is because if η increases continuously taking values from 1 onwards, these two roots remain in the interval $(\widehat{x}, 1)$ until $\eta = 1.3615345$ when they both coincide with the double root ξ.

From the value $\eta = 1.3615345$ onwards the two roots become a pair of complex conjugate ones.

Since $\beta_1(\omega)$ is an increasing function at $\omega = 1$, it will be increasing in a neighborhood of 1. So, by increasing ω continuously from 1 to $\widehat{\omega}$ we will pass first through a value of ω, let it be denoted by $\omega\prime$, which will correspond to the local maximum of $\beta_1(\omega)$ and then through a value of ω corresponding to the local minimum.

The previous discussion leads to the conclusion that the optimal value of $\omega \in (1-\frac{1}{\sqrt{\eta}}, \widehat{\omega}]$, let it be ω^*, will be given by that value of the pair $\{\omega\prime, \widehat{\omega}\}$ that maximizes $\beta_1(\omega)$. From a variety of numerical experiments we can come up with the conjecture that ω^* is the optimal value for all $\omega \in (1-\frac{1}{\sqrt{\eta}}, 1+\frac{1}{\sqrt{\eta}})$.

By putting in (4.3) $\widehat{\omega}$ for ω and $\widehat{\eta}$ for η in (4.1) we obtain

$$\begin{aligned}\beta_1(\widehat{\omega}) = \ & \frac{\left[(3-\widehat{\omega})-\left[(2-\widehat{\omega})^2+(\widehat{\omega}-1)\right]^{\frac{1}{2}}\right]}{(2-\widehat{\omega})^2\widehat{\omega}^3\left[-(2-\widehat{\omega})+\left[(2-\widehat{\omega})^2+(\widehat{\omega}-1)\right]^{\frac{1}{2}}\right]} \\ & \times \frac{(1-\widehat{\omega})^3}{\left[-1+\left[(2-\widehat{\omega})^2+(\widehat{\omega}-1)\right]^{\frac{1}{2}}\right]} =: g(\widehat{\omega}).\end{aligned} \tag{4.6}$$

It is readily seen that $g(\omega)$, defined in (4.6), is a continuous function of $\omega \in (1,2)$. By differentiating $g(\omega)$ and studying the sign of its derivative it can be found after a long but elementary algebraic manipulation takes place that $\frac{dg(\omega)}{d\omega}$ is positive in $(1,2)$ with $\lim_{\omega\to 1^+} g(\omega) = 0$ and $\lim_{\omega\to 2^-} g(\omega) = \frac{27}{32}$. Therefore $g(\omega)$ is a strictly increasing function in $[1,2)$ which implies that for $\rho(B^3) \in (1, \frac{27}{32})$ there is **no** $\widehat{\omega}$ such that $\beta_1(\widehat{\omega}) = \rho(B^3)$. This constitutes one of the main differences of the special case $p = 3$ from the general case $p \geq 4$. Obviously, in the present case $\omega^* = \omega\prime$.

After the analysis so far as well as the preceding one it can be concluded that there is an interval of η for $\eta > 1$ such that $\omega^* = \omega\prime$. This interval is a left subinterval of $(1, 1.361534)$. From various numerical experiments we have observed that the subinterval in question is large compared to a small right subinterval of $(1, 1.361534)$ for which $\omega^* = \widehat{\omega}$. For values of $\eta > 1.361534$, $\widehat{\omega}$ remains the optimal value for ω.

4.2 Nonpositive Case

For the boundary curve $\gamma_1(\omega)$, defined in $[\widetilde{\omega}, \widehat{\widehat{\omega}}]$, we have exactly the same conclusions as the ones in the general case. So, from (3.12) we take

$$\gamma_1(\omega) = \frac{[1+(1-\omega)^2\eta]^3}{(2-\omega)^2\omega^3\eta[1-(1-\omega)\eta]}. \tag{4.7}$$

The behavior of the curve $\gamma_2(\omega)$ defined in $(\widehat{\widehat{\omega}}, 1+\frac{1}{\sqrt{\eta}})$ is also the same as that of the general case. In the present case, however, we will find an analytic form of this curve by

proving that it is derived from $z(\eta e^{i\theta})$ at $\theta = 0$.
For this, we prove first that the intersection points of the curve $z(\eta e^{i\theta})$ with the real axis for $\theta \neq 0, \pi$ are at most one. We consider the imaginary part of $z(\eta e^{i\theta})$ and set it equal to zero, namely $\mathrm{Im} z(\eta e^{i\theta}) = 0$, to find the values of θ that correspond to the points of interest. After some simple algebraic manipulation we obtain the known values $\theta = 0$ and $\theta = \pi$ and also the following equation in θ

$$cos\theta = -\frac{(1-\omega)^7\eta^4 - 3(1-\omega)^3(2-\omega)\eta^2 + 1}{2(1-\omega)\eta[1+(1-\omega)^5\eta^2]}. \tag{4.8}$$

In the case where the right hand side of (4.8) is outside the closed interval $[-1, 1]$ there is no θ satisfying (4.8). This is, of course, the case that corresponds to values of ω in the interval $(\widetilde{\omega}, \widehat{\omega})$ and this is because the function $z(\eta e^{i\theta})$ is conformal in the interval in question. In the cases $cos\theta = 1$ or -1 we obtain the values $\theta = 0$ and $\theta = \pi$ which we have excluded. However, if in (4.8) $cos\theta \in (-1, 1)$ then we obtain two solutions in $(0, 2\pi)$ that give the same intersection point with the real axis because of the symmetry of the curve $z(\eta e^{i\theta})$ *wrt* this axis. Since both points $z(\eta e^{i\theta})$ at $\theta = 0$ and $\theta = \pi$ belong to the real negative semiaxis for $\omega \in (1 + \frac{1}{\eta}, 1 + \frac{1}{\sqrt{\eta}})$, the intersection point in question will belong to the real positive semiaxis. So, the curve $\gamma_2(\omega)$ is obtained from $z(\eta e^{i\theta})$, for $\theta = 0$, and is therefore given by

$$\gamma_2(\omega) = \frac{[1-(1-\omega)^2\eta]^3}{(2-\omega)^2\omega^3\eta[1+(1-\omega)\eta]}. \tag{4.9}$$

Setting $x = 1 - \omega$ and differentiating (4.9) *wrt* ω we find out that $\gamma_2\prime(\omega)$ has the same sign as the function $f(x; \eta)$ of (4.4). The study of $f(x; \eta)$ made in the present nonpositive case reveals that $\gamma_2\prime(\omega)$ is a strictly decreasing function. The value of ω for which $\gamma_1(\omega) = \gamma_2(\omega)$, denoted by $\widehat{\omega}$ is the unique real root of the equation

$$\eta^4 x^7 + 3\eta^2 x^4 + 3\eta^2 x^3 + 1 = 0, \quad x = 1 - \omega \tag{4.10}$$

in the interval $(1 + \frac{1}{\eta}, 1 + \frac{1}{\sqrt{\eta}})$.

It remains to study the behavior of the curve $\gamma_3(\omega)$ in the interval $(1 - \frac{1}{\sqrt{\eta}}, \widetilde{\omega})$.

From the analysis in [12] we know that the behavior of this curve for $\eta = 1$, and $p = 3$, is different from that of the general case $p \geq 4$. Obviously, based on continuity arguments we can claim that the behavior of the curve $\gamma_3(\omega)$ for $\eta > 1$ in a neighborhood of 1 will still be different from the one in the general case $p \geq 4$.

The curve $\gamma_3(\omega)$ can be given analytically provided one plugs in the value of θ from (4.8) in the real part of $z(\eta e^{i\theta})$. However, this analytic expression is rather complicated and is not given here. The study of the behavior of $\gamma_3(\omega)$ based on its analytic form is even more complicated. So, what we did was to make a number of numerical experiments as this was done in the general case $p \geq 4$. From this study strong numerical evidence supports the

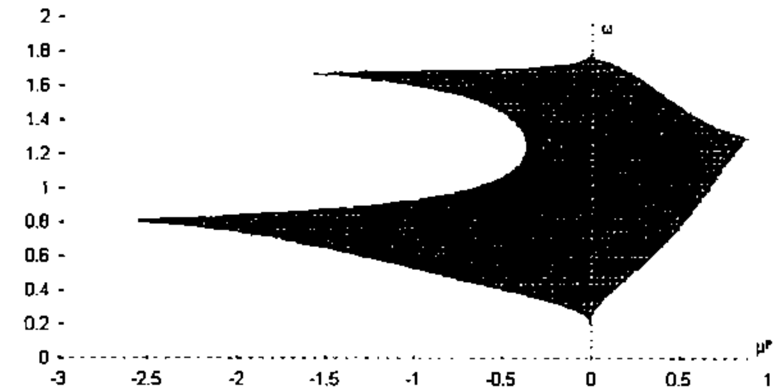

Figure 4: Convergence Region of the General Case

conjecture that for an interval of $\eta > 1$ there is a value of ω, denoted by $\tilde{\tilde{\omega}}$, corresponding to the maximum value of $\gamma_3(\omega)$ and such that $\gamma_3(\tilde{\tilde{\omega}}) > \gamma_3(\hat{\omega})$.

The above analysis for the curves $\gamma_1(\omega)$ and $\gamma_2(\omega)$ and the numerical experiments for the curve $\gamma_3(\omega)$ support our claim that the optimal value of $\omega \in (1 - \frac{1}{\sqrt{\eta}}, 1 + \frac{1}{\sqrt{\eta}})$, denoted by ω_{opt}, is one of the triad $\{\tilde{\omega}, \hat{\hat{\omega}}, \tilde{\tilde{\omega}}\}$ that maximizes the corresponding value for the boundary curve.

5 Numerical Examples and Concluding Remarks

A number of numerical examples run on a computer are illustrated in Tables 1 and 2 for $p = 4$ and $p = 3$, respectively, for the selected values of η shown there. In each case, based on the theory developed in this paper a systematic search was made considering all values of $\omega = 0.00001(0.00001)1.99999$ to find the one for which $\rho(B)$ was taking the largest possible value. The corresponding ω appears as ω_{opt} in both Tables. Then, we worked the other way around. Namely, for each computationally obtained ω_{opt} and using the value of $\rho(B)$ that was found we computed the corresponding value of η. The values of η that we obtained were very close to the ones originally considered. Some minor discrepancies can be attributed to the presence of the round–off errors and the final effect of their propagation during the many complicated computations involved.

Some of the results in the Tables are depicted in Figures 4 and 5. Figure 4, that is a good representative of the general case, is the "*union*" of Figures 2 and 3 in the (μ^4, ω)–plane and shows the region of convergence for $p = 4$ and $\eta = 1.5$. Figure 5 depicts both the nonnegative and nonpositive cases in the (μ^3, ω)–plane, in the special case $p = 3$, for the values of $\eta = 1,\ 1.1,\ 1.5$ and 3. The outmost curves correspond to $\eta = 1$ and the inmost ones to $\eta = 3$.

It should also be noted that in all the Figures 2–5 the lower parts of the graphs tend to

Table 1: *Case* $p = 4$

		NONNEGATIVE		NONPOSITIVE	
η	$\rho(S_\omega)$	ω_{opt}	$\rho(B)$	ω_{opt}	$\rho(B)$
1.01	.990099	1.75757	.999825	1.99010	7.08862
1.025	.975610	1.68152	.999397	1.97562	4.50044
1.05	.952381	1.61069	.998455	1.95242	3.20247
1.1	.909091	1.52737	.996048	1.90946	2.29492
1.2	.833333	1.43243	.990037	1.83559	1.66714
1.3	.769231	1.37312	.983163	1.77491	1.39772
1.4	.714286	1.33046	.975863	.798640	1.30969
1.5	.666667	1.29762	.968374	.810338	1.27384
1.7	.588235	1.24954	.953348	.830029	1.21361
2.0	.5	1.20194	.931606	.852860	1.14327
2.5	.4	1.15401	.898763	.879690	1.05839
3.0	.333333	1.12473	.870202	.898198	.997075
4.0	.25	1.09054	.823413	.922104	.911813
5.0	.2	1.07113	.786582	.936897	.853412
7.5	.133333	1.04634	.720355	.957192	.760582
10.0	.1	1.03438	.674892	.967603	.702961
15.0	.066667	1.02268	.613961	.978201	.630867
20.0	.05	1.01692	.573289	.983574	.585088

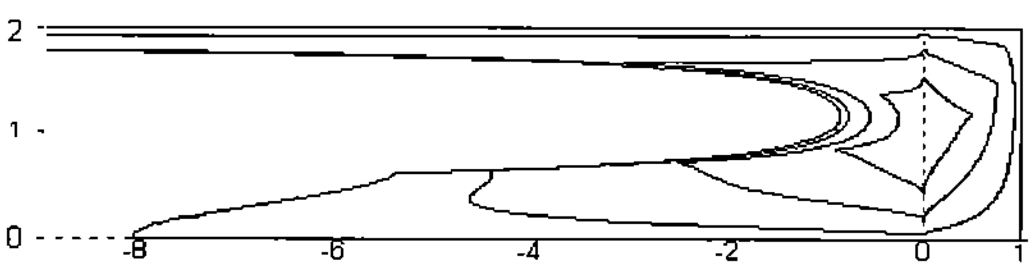

Figure 5: Special Case $p = 3$

Table 2: *Special Case* $p = 3$

η	$\rho(S_\omega)$	NONNEGATIVE		NONPOSITIVE	
		ω_{opt}	$\rho(B)$	ω_{opt}	$\rho(B)$
1.01	.990099	1.26900	.997136	1.99010	17.1565
1.025	.975610	1.27165	.992923	1.97561	9.36077
1.05	.952381	1.27557	.986118	1.95241	5.94629
1.1	.909091	1.28365	.973273	1.90928	3.80861
1.2	.833333	1.30430	.950393	1.83453	2.47910
1.3	.769231	1.34056	.930999	1.77235	1.95270
1.35	.740741	1.57051	.926279	1.74510	1.78910
1.4	.714286	1.53721	.922066	1.72004	1.66121
1.5	.666667	1.48141	.913304	1.67549	1.47288
1.6	.625	1.43650	.904326	1.63711	1.33959
1.7	.588235	1.39953	.895315	.753809	1.26847
2.0	.5	1.31945	.868976	.785997	1.16686
3.0	.333333	1.19317	.794799	.850643	.966230
4.0	.25	1.13894	.739067	.885159	.855411
5.0	.2	1.10859	.695786	.906677	.782029
7.5	.133333	1.07031	.619407	.936413	.669542
10.0	.1	1.05200	.568149	.951766	.602291
15.0	.066667	1.03420	.501097	.967467	.520972
20.0	.05	1.02548	.457471	.975455	.471012

the point $(0,0)$ as $\rho(B) \to 0^+$ while their upper parts tend to the point $(0,2)$. Both these points constitute singular points for all the graphs since, as is known, the SSOR method does not converge for $\omega = 0$ or 2.

Before we conclude this section we simply make one final point regarding the real spectra, $\sigma(B^p)$, case. From the analysis of the nonnegative and the nonpositive cases of this paper and the examples illustrated in Figures 4 and 5 there is a strong indication that if one can adopt a kind of a trial and error procedure one may be able to find, at least computationally, the solution to the problem in the real spectra case.

References

[1] Berman A. and R.J. Plemmons, *Nonnegative Matrices in the Mathematical Sciences*, SIAM, Philadelphia, 1994.

[2] D'Sylva E. and G.A. Miles, The S.S.O.R. Iteration Scheme for Equations with σ_1–Orderings, *Comput. J.*, **6**, 1963, pp. 271–273.

[3] Eiermann M., W. Niethammer and A. Ruttan, Optimal Successive Overrelaxation Iterative Methods for p–Cyclic Matrices, *Numer. Math.*, **57**, 1990, pp. 593–606.

[4] Galanis S., A. Hadjidimos and D. Noutsos, On Different Classes of Monoparametric Stationary Iterative Methods for the Solution of Linear Systems, *Math. Comput. Simulation*, **28**, 1986, pp. 115–128.

[5] Galanis S., A. Hadjidimos and D. Noutsos, On the Convergence of Monoparametric k–Step Euler Methods for the Solution of Linear Systems, *Intern. J. Computer Math.*, **26**, 1988, pp. 45–56.

[6] Galanis S., A. Hadjidimos and D. Noutsos, On the Equivalence of k–Step Iterative Euler Methods and Successive Overrelaxation (SOR), *Math. Comput. Simulation*, **30**, 1988, pp. 213–230.

[7] Galanis S., A. Hadjidimos and D. Noutsos, On an SSOR Matrix Relationship and Its Consequences, *Comput. Methods Appl. Mech. Engrg.*, **27**, 1989, pp. 559–570.

[8] Hadjidimos A., X.-Z. Li and R. S. Varga, Application of the Schur–Cohn Theorem to Precise Convergence Domains for the Cyclic SOR Iterative Method, unpublished manuscript, 1985.

[9] Hadjidimos A. and M. Neumann, Precise Domains of Convergence for the Block SSOR Method Associated with p–cyclic Matrices, *BIT*, **29**, 1989, pp. 311–320.

[10] Hadjidimos A. and M. Neumann, Convergence Domains of the SSOR Method for a Class of Generalized Consistently Ordered Matrices, *J. Comp. Appl. Math.*, **33**, 1990, pp. 35–52.

[11] Hadjidimos A. and D. Noutsos, The Young–Eidson Algorithm: Applications and Extensions, *SIAM J. Matrix. Anal. Appl.*, **11**, 1990, pp. 620-631.

[12] Hadjidimos A., D. Noutsos and M. Tzoumas, On the Exact p-Cyclic SSOR Convergence Domains, *Linear Algebra Appl.*, **232**, 1996, pp. 213–236.

[13] Hadjidimos A. and R. J. Plemmons, A General Theory of Optimal p–Cyclic SOR, *Numer. Math.*, **67**, 1994, pp. 475–490.

[14] Henrici P., *Applied and Computational Complex Analysis*, Wiley, New York, 1974.

[15] Kontovasilis K., R. J. Plemmons and W. J. Stewart, Block Cyclic SOR for Markov Chains with p–Cyclic Infinitesimal Generator,, *Linear Algebra Appl.*, **154–156**, 1991, pp. 145–223.

[16] Kredell B., On Complex Successive Overrelaxation, *BIT*, **2**, 1961, pp. 143–152.

[17] Lynn M.S., On the Equivalence of SOR, SSOR and USSOR as Applied to σ_1–Ordered Systems of Linear Equations, *Comput. J.*, **7**, 1964, pp. 72–75.

[18] Neumaier A. and R.S. Varga, Exact Convergence and Divergence Domains for the Symmetric Successive Overrelaxation (SSOR) Iterative Method Applied to H–Matrices, *Linear Algebra Appl.*, **58**, 1984, pp. 261–272.

[19] Niethammer W., Relaxation bei Matrizen mit der Eigenschaft "A". *Z. Angrew. Math. Mech.*, **44**, 1964, pp. T49–T52.

[20] Niethammer W., J. dePillis and R.S. Varga, Convergence of Block Iterative Methods Applied to Sparse Least–Squares Problems. *Linear Algebra Appl.*, **58**, 1984, pp. 327–341.

[21] Niethammer W. and R.S. Varga, The Analysis of k–Step Iterative Methods from Summability theory, *Numer. Math.*, **41**, 1983, pp. 177–206.

[22] Noutsos D., Optimal Stretched Parameters for the SOR Iterative Method. *J. Comp. Appl. Maths*, **48**, 1993, pp. 293–308.

[23] Varga R.S., p–Cyclic Matrices: A Generalization of the Young–Frankel Scheme, *Pacific J. Math.*, **9**, 1959, pp. 617–628.

[24] Varga R.S., *Matrix Iterative Analysis*, Prentice Hall, Englewood Cliffs, NJ, 1962.

[25] Varga R.S., W. Niethammer and D.-Y. Cai, p–Cyclic Matrices and the Symmetric Successive Overrelaxation Method, *Linear Algebra Appl.*, **58**, 1984, pp. 425–439.

[26] Wild P. and W. Niethammer, Over and Underrelaxation of Linear Systems with Weakly Cyclic Jacobi Matrix of Index p, *Linear Algebra Appl.*, **91**, 1987, pp. 29–52.

[27] Young D.M., Iterative methods for solving partial differential equations of elliptic type, *Trans. Amer. Math. Soc.*, **76**, 1954, pp. 92–111.

[28] Young D.M., *Iterative Solution of Large Linear Systems*, Academic Press, New York, NY, 1971.

[29] Young D. M. and H.E. Eidson, On the Determination of the Optimum Relaxation Factor for the SOR Method When the Eigenvalues of the Jacobi Matrix are Complex, Report CNA–1, Center for Numerical Analysis, University of Texas, Austin, Texas, 1970.